

Dating of marine sediments and time evolution of heavy metal concentrations in the Bay of Cádiz, Spain

R.A. Ligeró^{a,*}, M. Barrera^a, M. Casas-Ruiz^a, D. Sales^b, F. López-Aguayo^c

^aDepartment of Applied Physics, University of Cádiz, C.A.S.E.M 11510, Puerto Real, Cádiz, Spain

^bDepartment of Environmental Technology, University of Cádiz, C.A.S.E.M 11510, Puerto Real, Cádiz, Spain

^cDepartment of Geology, University of Cádiz, C.A.S.E.M 11510, Puerto Real, Cádiz, Spain

Received 10 March 2001; accepted 30 July 2001

“Capsule”: *Heavy metals in the Bay of Cadiz, Spain have increased in the twentieth century.*

Abstract

In this paper the time evolution of heavy metal concentration of Pb, Zn, Cd and Hg, in the sediments of the Bay of Cádiz (southwest of Spain) is studied during the past century, as a result of the industrial influence in the zone. The study has been performed using sedimentary profiles that have been extracted from the seabed. The measurement of ²¹⁰Pb and ¹³⁷Cs radionuclides has provided the dating of the sediment layers, up to a depth corresponding to the age of 115 years. The relative sedimentation rates obtained are around 0.2 cm/year. The ¹³⁷Cs activity profile reflects the concentration of this radionuclide in the atmosphere and into aquatic systems during the second half of the twentieth century. This profile has been used to ratify the results provided by the ²¹⁰Pb dating method. © 2002 Elsevier Science Ltd. All rights reserved.

Keywords: Heavy metals pollution; Dating by ²¹⁰Pb; Seabed sediments; Nuclear spectrometry; Time evolution

1. Introduction

The Bay of Cadiz (southwest of Spain) is a singular geographical zone, due to its ecological, economic, tourist, social and cultural values. Its current configuration is the result of a natural evolution conditioned by some geological agents (coastal dynamics, the Guadalete river mouth, the San Pedro tidal channel and the meteorological conditions, among others), biological factors (the vegetation and the fauna), and a strong human alteration of the environment (the traditional salt mines, the fish factories and the development of the metropolitan area). It is an environment where autochthonous elements, like the sea, the marshes, the beaches and the pine-groves coexist with several urban nucleus, and transport infrastructures as well as harbours and tourist facilities.

Normally, three zones are distinguished in the Bay of Cádiz (Fig. 1): The Maritime Bay, the Terrestrial Bay

and the Amphibious Bay (Barragán, 1995, 1996). The former one, which was declared Natural Protected Space in 1989 (Natural Park of the Bay of Cadiz), consists of intertidal zones constituted by natural marshes and saline pits. The Terrestrial Bay is constituted by consolidated coastal lands where the Bay of Cádiz metropolitan area is located, which includes five towns (Cádiz, San Fernando, Puerto Real, Puerto de Santa María and Rota), and whose population exceeds 400,000 inhabitants.

The Maritime Bay consists of two zones:

1. The Outer Bay, that is extended northward from the bridge José Leon de Carranza up to Rota. This zone of the Bay is the most exposed to the surge, tidal currents and the west wind. The bottom is composed by sandy and muddy sediments, with a rock substratum of Pliocene age. The Guadalete River, the most important source of sediments, and the main tidal narrow channel, San Pedro River, empty in this area.
2. The Inner Bay is located to the south of the bridge. Its relative isolation protects it from the surge and,

* Corresponding author. Tel.: +34-956-016068; fax: +34-956-016079.

E-mail address: rufino.ligeró@uca.es (R.A. Ligeró).

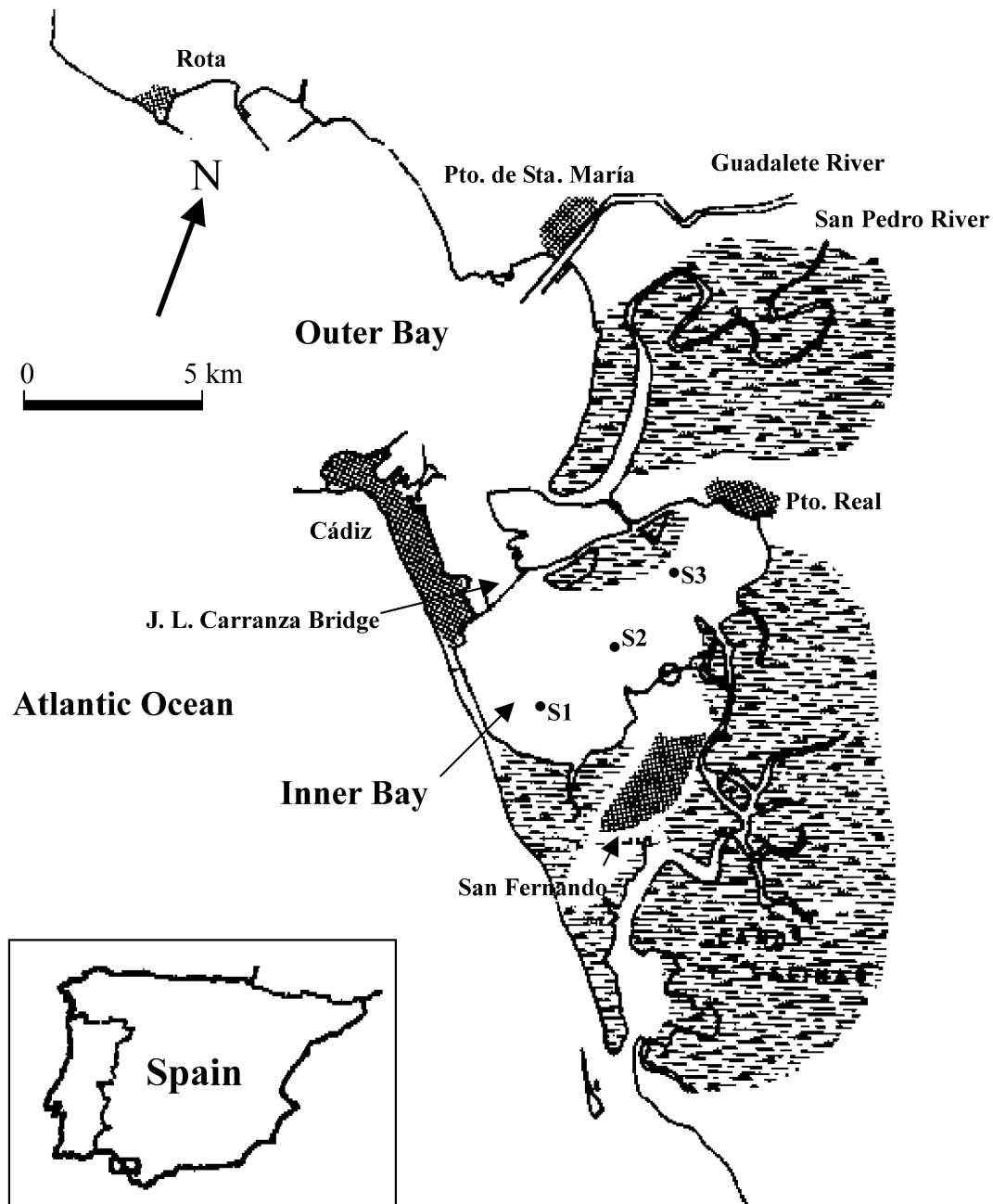


Fig. 1. The Bay of Cadiz and the sampling stations.

partially, the wind. So, the water dynamics in this area are almost exclusively of tidal nature, which allows the accumulation of small grain size sediments (silts and clays). These grain size characteristics provide the sediment with a great absorption capacity of the elements and substances solved in the water, and therefore turn this region into a potential reservoir of the toxic wastes dumped into the environment. It must be emphasized (Fig. 1) that several towns are located in the area of the Inner Bay, as well as the Natural Park of the Bay, so it is necessary to evaluate the influence that the

demographic and industrial activities have on this region of high ecological value. Because of the aforementioned reasons, this study concerns the Inner Bay.

The aim of this work is to investigate the evolution experimented by the concentration of the heavy metals Pb, Zn, Cd and Hg in the seabed sediments of the inner Bay of Cadiz during the last century. However, the dating techniques used allow us the extrapolation of the results for the last 300 years. The main dating technique applied in this work is the ^{210}Pb method, which is based on the incorporation of the former

radionuclide into the sediments, as a consequence of the ^{222}Rn radioactive decay. The radon is emanated, as a product of the ^{226}Ra radioactive disintegration, from the crust of the earth towards the atmosphere. The ^{210}Pb incorporated decays with a half-life of 22.3 years, so that its activity shows a diminishing profile with the depth in an undisturbed sedimentary environment.

To check the results obtained through the application of this method, the concentration of ^{137}Cs has also been measured; this is an artificial radionuclide introduced in the environment since 1954, due mainly to the nuclear weapon tests. The activity of this radionuclide reached a maximum in the years 1962–1963, because of the increase of the earlier mentioned nuclear tests. More recent events, such as the disaster of the nuclear reactor of Chernobyl, in 1986, threw into the environment a great amount of this element. So, the profile of ^{137}Cs in the sediments must show the incorporation of this radionuclide to the environment, as well as the mentioned maxima of concentration. This fact can be used as an alternative method for dating the sediments accumulated over the last 50 years (Pinglot and Pourchet, 1995; Callaway et al., 1996). Nevertheless, due to the behaviour of the ^{137}Cs in the aquatic systems, this technique has serious limitations. On the one hand, this element has a long residence time in the marine water. This fact can delay the incorporation of the ^{137}Cs into the sediment, and then, can provoke a displacement of the maxima in the profile towards more superficial levels. On the other hand, the great mobility of this element in the sedimentary column can cause the diffusion of the element towards deeper sediment layers (Davis et al., 1984; Abril et al., 1992).

The evaluation of the sedimentation rate requires the determination of the water content in the sediments, as corrections due to the compactness must be made. From the knowledge of the water content profile, together with the organic carbon profile, a classification of the stations can be derived, according to their grain size, which provides useful information on the sedimentary environment for each sampling station.

2. Materials and methods

Three sampling stations, S1, S2 and S3 (Fig. 1), have been selected, representing the behaviour of the sediments in the zone, and a cylindrical sediment core extracted from each station has been studied. The tidal dynamics in the Inner Bay have an asymmetrical behaviour, as it is more intense to the north and decreases southward of the Bay. Therefore, a grain size gradient is established and, as a result, the smaller grain size sediments follow this trend. Furthermore, the flow and reflux dynamics of tides create an east–west stream

(Consejería de Agricultura y Pesca Andalusian Govern, 1994). Thus, a relative southwest–northeast direction has been selected for the sampling stations, which are separated by nearly 3 km.

The sediment samples, contained in cylindrical aluminium pipes of 1 m length and 6 cm inner diameter, are taken out from the seabed by a Lanesky vibrocore system that allows the column to be obtained without alteration in the structure of the sediment. In order to assure the immobilization of the core and the preservation of the interstitial water, previous to the sample preparation, the pipes were cooled at $-10\text{ }^{\circ}\text{C}$. Afterwards, the sediment profiles were cut into 2-cm thick slices, up to a depth of 54–56 cm which, as we will see, is enough to reach the base levels.

The sediment slices were dried at a temperature of $55\text{ }^{\circ}\text{C}$ during 48 h, in order to eliminate completely the water content of the sediment. This temperature is low enough to avoid the loss of volatile elements like ^{210}Po and Hg that will be measured later. The loss of weight after the drying determines the water content of the sediment, $w(\%)$, which is necessary to apply a correction for compactness and, consequently, to evaluate the sedimentation rates.

The sediments were crushed and sieved to a grain size smaller than $500\text{ }\mu\text{m}$, to obtain the sample homogeneity. Three 1-g aliquots have been separated from each sample to determine the organic carbon content, the ^{210}Pb activity and heavy metal concentrations. The rest of the sample was used to perform the gamma spectrometric measurements.

The organic carbon (OC) content has been evaluated applying a modification of the technique of Gaudette et al. (1974) developed by El-Rayis (1985), which consists in the oxidation of the sediment sample with potassium dichromate in a concentrated acid medium at $135\text{ }^{\circ}\text{C}$ temperature. The OC content is obtained by tritiation with ferrous ammonium sulfate of the excess of dichromate after oxidation. The percentage of OC detected by this method depends on the type of sediment and ranges between 80 and 95%. The elemental carbon stands unaltered, and the carbonates do not present interference problems.

The heavy metals Pb, Cd and Hg were determined by Atomic Absorption Spectrometry (AAS), and Zn was measured by Atomic Emission Spectrometry with Inductively Coupled Plasma (ICP-AES).

Pb was measured using an AAS 939-UNICAM with a slotted tube atom trap (STAT), incident radiation with a wavelength of 217.0 nm, a slit of 0.5 nm and a limit of detection of 0.04 mg/l.

Cd was determined with an AAS 900-Phillips with graphite furnace, electrothermic spray chamber, PU 9390X, and furnace autosampler, PU 9380. The wavelength was 228.8 nm with 0.5 nm of slit and 0.3 $\mu\text{g/l}$ as limit of detection.

Zn was determined with a ICP PHILLIPS PU 7000, using 213.856 nm as wavelength and 4.1 µg/l as limit of detection.

Hg was measured using an AAS 939-UNICAM with cold vapour module, UNICAM VP 90, wavelength of 253.7 nm, slit of 0.7 nm and 0.87 mg/l as limit of detection.

To validate the results a reference material, MESS-1, was used in the different determinations.

To extract the metals, the sediment sample was subjected to an acid digestion (Sturgeon et al., 1982). High purity reagents were used, and the free metals water (bi-distilled). The relative accuracy in the determination of the metal concentrations is around 5%.

The determination of the ^{210}Pb has been accomplished by measuring the concentration of its daughter, ^{210}Po , by alpha spectrometry. The half-life of the former radionuclide is 135 days, so that the secular equilibrium between lead and polonium in sediments is expected to be older than 2 years. The measurement of ^{210}Po has been effected by the detection of its 5.305 MeV particle emission, using the tributylphosphate method (TBP). This method consists of a sediment digestion, the separation of the polonium by TBP and its autodeposition on silver plates. Later, it was made the measurement on such plates by an alpha spectrometric system (SOLOIST-U0450, EG&G ORTEC). The quantitative determination of ^{210}Po is made adding the artificial racers ^{208}Po and ^{209}Po , that are not found in natural form in the sediments, and whose subsequent detection in the alpha spectrum will indicate the overall efficiency of the measurement system and the polonium extraction process.

The gamma emitters ^{137}Cs and ^{226}Ra measurements were performed with a coaxial detector HPGe of 90 cm³ active volume, with a relative efficiency of 20% (with respect to a NaI(Tl) detector 3×3 inches) and a resolution of 2 keV, for 1332 keV. This detector is sensitive in the energetic range 50 keV–10 MeV. The samples were packed in cylindrical containers of 4.6 cm diameter, and were sealed during a month before their measurement with the purpose of assuring the secular equilibrium between ^{226}Ra and its daughter, ^{222}Rn . The determination of the ^{137}Cs has been performed through the detection of the 662 KeV photon and intensity 85%, emitted by its descendent in secular equilibrium, $^{137}\text{Ba}^m$. The measurement of the ^{226}Ra has been performed by the detection of the 352 KeV photon, and intensity 35%, emitted by ^{214}Pb , which is in secular equilibrium with ^{222}Rn and consequently with ^{226}Ra . The measurement system uses a 10-cm thick lead shielding, with interior 1-mm plates made of Cu and Cd, to minimize the external radiation. It was necessary to apply interference corrections for the 352 keV photon (^{226}Ra), but not for the 662 keV photon (^{137}Cs). The measurement of the environmental radiation background has been performed periodically. The efficiency of the equipment,

which is a function of the gamma radiation energy, the sample height, and the sediment density (Ramos-Lerete et al., 1998a; Barrera et al., 1999) was calibrated. To obtain meaningful statistics in the measurements, the time of spectrometry for each sample was 72 h.

3. Dating of sediments and sedimentation rates

The age of the sediments has been determined using the ^{210}Pb method, and the CRS (Constant Rate Supply) model (Appleby and Oldfield, 1983). According to this model, the flow of ^{210}Pb from the water system towards the sediment is considered constant, independently of the sedimentation rate (Dickinson et al., 1996). This technique uses the activity of the ^{210}Pb incorporated to the sediment (^{210}Pb “unsupported”) that is determined by subtracting from the total ^{210}Pb the fraction coming from the ^{226}Ra content in the sediment. As there is a small loss of ^{222}Rn , the secular equilibrium between ^{226}Ra and ^{210}Pb is broken. Therefore, in order to evaluate the activity of ^{210}Pb coming from the ^{226}Ra , instead of using the ^{226}Ra measured by gamma spectrometry, the ^{210}Pb average value of 10.5 ± 0.5 Bq/kg, measured in the deepest layers of the sedimentary column will be considered. The constant profile shown by the ^{226}Ra in all the stations allows us to state that its daughter, ^{210}Pb , must also be constant (since it is not probable for the emanation rate of the ^{226}Ra to change with the depth), and must be equal to the above mentioned value of 10.5 ± 0.5 Bq/kg. Therefore, the following relationship is verified in every layer of the three stations

$$^{210}\text{Pb}(\text{unsupported}) = ^{210}\text{Pb}(\text{total}) - 10.5 \text{ Bq/kg.}$$

Table 1 shows the ages obtained for the layers of the three stations when applying the CRS model, as well as the date assigned to the layers, which, considering the extraction date of the cores (July 1998), obeys the relationship $date = 1998 - age$. Since the half-life of ^{210}Pb is 22.3 years, the technique permits dating of a maximum age of 100–200 years. In this study, due to the experimental uncertainty in the determination of the Pb(unsupported), the dating has provided a maximum age of 115 years, corresponding to the layers of 18, 24 and 30 cm of depth for the stations S1, S2 and S3, respectively. Nevertheless, by taking into account the sedimentation rate of each station, the age of the deepest layers can be calculated by extrapolation, though the results are only approximate, since it is not possible to ensure that the sedimentation rate has been constant for a period of time longer than a century. Table 2 shows the values of r_m , the average mass sedimentation rate (the amount of mass accumulated by surface and time unit) and r_l , the average linear sedimentation rate (the sediment thickness accumulated by time unit). Considering the grain

Table 1
Age and date of sediments

z (cm)	S1		S2		S3	
	Age (years)	Date	Age (years)	Date	Age (years)	Date
0–2	2±0.3	1996±0.3	2±0.3	1996±0.3	3±1	1995±1
2–4	6±0.5	1992±0.5	6±1	1992±1	5±1	1993±1
4–6	13±1	1985±1	12±1	1986±1	8±1	1990±1
6–8	25±1	1973±1	19±2	1979±2	10±2	1988±2
8–10	41±2	1957±2	28±3	1970±3	14±2	1984±2
10–12	65±4	1933±4	38±4	1960±4	17±2	1981±2
12–14	73±4	1925±4	45±5	1953±5	23±3	1975±3
14–16	85±5	1913±5	52±7	1946±7	28±3	1970±3
16–18	107±8	1891±8	61±10	1937±10	32±3	1966±3
18–20	(125)	(1873)	72±14	1926±14	34±3	1964±3
20–22			87±23	1911±23	38±4	1960±4
22–24			111±30	1887±30	46±5	1952±5
24–26	(150)	(1848)	(120)	(1878)	61±7	1937±7
26–28					82±12	1916±12
28–30					115±27	1883±27
30–32	(200)	(1798)	(150)	(1848)	(125)	(1873)
32–34						
34–36						
36–38	(230)	(1768)	(180)	(1818)	(150)	(1848)
38–40						
40–42						
42–44	(270)	(1728)	(210)	(1788)	(170)	(1828)
44–46						
46–48						
48–50	(310)	(1688)	(235)	(1763)	(200)	(1798)
50–52						
52–54						
54–56	(350)	(1648)	(270)	(1728)	(220)	(1778)

Table 2
Sedimentation rates and ^{210}Pb inventories

	S1	S2	S3
r_m (mg/cm ² year)	89±6	139±37	204±40
r_l (cm/year)	0.16±0.01	0.22±0.06	0.27±0.06
P (mBq ^{210}Pb /cm ² year)	3.2±0.1	5.4±0.2	2.5±0.2

size analysis that is accomplished in the following section, it can be appreciated that the sedimentation increases as the grain size is bigger. Since the transport and subsequent sedimentation of this coarse sediment and particles is due to a high energy in the environment, we can state that there is a greater sedimentation as the marine dynamics of the environment increase.

Table 2 includes the ^{210}Pb flow values onto the sedimentary profiles, the so-called ^{210}Pb inventory, which is deduced from the ^{210}Pb (unsupported) profile. The ^{210}Pb inventory values are equal to or smaller than the average value of the atmospheric ^{210}Pb flow on the zone (5–10 mBq cm⁻²year⁻¹), what indicates that there is a loss of ^{210}Pb in the transfer of such radionuclide from the atmosphere to the sediment. This could also be due to the dynamics of the environment, and then, an excess of

^{210}Pb would have to be accumulated on quiet hydrodynamics zones.

From the CRS dating model, a sedimentation rate is also derived for each layer of the stations, so it is possible to study the evolution of the sedimentation rate versus the time. Since the main hypothesis of the model is that the ^{210}Pb flow towards the sediments is constant, a low concentration of this radionuclide in the superficial layers would be explained in terms of a fast recent sedimentation (Clifton et al., 1994). However, as will be seen later, the superficial effect is linked to the dynamics of interface processes, and therefore the rigorous sediment dating would require another model, taking account of this interface process. Such a model would assume the existence of a superficial region of finite thickness, where all the ^{210}Pb incorporated into the sediment, would be accumulated. The CRS model can be considered as a limit case of this kind of model, in which such thickness is zero. In order to check the influence of this interface phenomenon on the sediment dating, the age of the layers has been evaluated again, using the same CRS model, but substituting the value of the ^{210}Pb activity in the superficial layers by a greater value, obtained by extrapolation of the exponential trend shown by the concentration profile of the

radioelement in the deepest levels. In this way, the elimination of the interface phenomena is simulated. The obtained results provide an identical dating to the one provided by the previous method. Therefore, it is concluded that the existence of the interface phenomena does not affect the dating of the sediment layers.

4. Results

4.1. Profile of experimental parameters

Tables 3 and 4 show the values of the measured parameters in the successive layers of the studied cores of sediments. The water content w has been measured in all the layers, and the other parameters have been determined in one of each three levels. To optimize the dating, the measurements of the radionuclide activities have been performed in every layer within the first 20 cm of the sediments, which is the zone where ^{137}Cs is accumulated. Fig. 2 shows the profiles of the variables w , OC, ^{210}Po , ^{137}Cs , and ^{226}Ra , for all the stations, and Fig. 3 shows the profiles corresponding to the heavy metals Zn, Pb, Cd and Hg. Below, the shape of these profiles is discussed.

4.1.1. Water content

The value of w is within the interval 35–70%, decreasing as the depth increases in all the stations. This fact is known as the *compactness of the sediment*, and is due to the pressure of the sedimentary column over each layer due to the depth increase. Furthermore, for a constant sedimentation, the deepest layers contain a quantity of sediment accumulated during a period of time greater than the corresponding to the superficial layers. Then, instead of the depth z , the calculations are effected with the mass depth $m(z)$, defined as the amount of sediment by surface unit of the column above such level. Also, it is used the mass sedimentation rate, r_m , defined as the sediment mass flow, which is meaning the quantity of mass accumulated by surface and time unit.

A decreasing profile $w(z)$, together with the high value of the parameter, suggests that the sedimentation takes place in a low dynamic marine environment, where there are no meaningful horizontal transport phenomena. It is appreciated that the station S3 has the smallest value of w as well as the softest decrease of this parameter. The station S1 shows the greatest values of w and station S2 has an intermediate behaviour, so that it is possible to establish an energy gradient of the marine environment ($S1 < S2 < S3$). Consequently, the grain size

Table 3
 w , O.C., ^{210}Pb , ^{137}Cs , ^{226}Ra

z (cm)	w (%)			OC (%)			^{210}Po (Bq/kg)			^{137}Cs (Bq/kg)			^{226}Ra (Bq/kg)		
	S1	S2	S3	S1	S2	S3	S1	S2	S3	S1	S2	S3	S1	S2	S3
0–2	72.7	63.9	52.8	4.53	3.72	2.42	18.4±1.1	25.0±1.5	17.4±1.3	7.1±0.8	5.2±1.1	0.79±0.25	14.1±2.2	15.4±3.3	17.9±2.5
2–4	69.0	61.8	53.1				27.3±1.3		15.1±1.2	7.7±1.3	7.0±1.2	0.67±0.35	14.2±3.3	13.4±3.0	19.0±3.2
4–6	69.7	58.7	55.3						30.2±2.0	8.2±1.1	5.4±1.0	0.69±0.27	14.1±2.8	14.4±3.0	17.7±2.2
6–8	66.6	53.4	53.9	5.05	4.01	2.11	36.3±3.0	30.8±1.7	15.9±1.6	7.3±1.2	4.8±1.1	1.02±0.29	14.0±3.1	15.8±3.3	18.8±2.8
8–10	64.7	50.8	51.0							4.7±1.0	0.9±0.6	0.87±0.34	11.4±2.7	16.3±2.8	15.7±2.7
10–12	61.5	52.3	53.0				25.9±1.4	24.8±1.4	15.7±1.5	4.5±1.0	0.8±0.5	0.83±0.39	10.1±2.5	18.8±2.7	18.4±3.3
12–14	57.3	52	50.4	4.54	4.01	2.08	13.1±0.7	18.5±1.2	17.1±1.4	4.7±0.7	1.3±0.5	1.18±0.27	15.4±2.4	17.4±2.6	16.6±2.4
14–16	55.5	52.4	48.1							2.3±0.7	<0.5	<0.5	17.9±2.9	15.9±2.5	18.5±3.0
16–18	54.4	50.1	46.2							2.10.7	<0.5	<0.5	13.3±2.5	16.9±2.5	21.5±3.0
18–20	55.1	50.3	45.2	4.2	3.6	2.02	13.6±0.7	16.4±1.0	12.6±1	<0.5	<0.5	<0.5	15.9±2.6	16.6±2.6	18.7±2.4
20–22	54.8	51.2	44.6												
22–24	56.4	49.5	45.3												
24–26	52.2	49.7	43.6	3.62	3.16	1.95	10.9±1.2	15.0±0.8	16.1±1.3	<0.5	<0.5	<0.5	15.1±2.5	19.1±3.2	18.0±2.5
26–28	50.5	50.1	43.8												
28–30	45.3	49.1	42.6												
30–32	41.8	51.1	41.6	2.37	3.43	2.2	11.5±1.1	11.5±1.0	13±0.9	<0.5	<0.5	<0.5	14.4±2.0	17.8±2.5	18.7±2.3
32–34	44.5	48.8	42.4												
34–36	44.9	45.6	42.8												
36–38	45.0	44.9	41.5	2.69	2.47	2.04	11.5±1.1	12.0±0.8	12.2±1	<0.5	<0.5	<0.5	15.8±1.9	15.8±2.5	19.4±2.3
38–40	44.8	40.0	41.9												
40–42	46.4	41.3	43.2												
42–44	46.4	41.1	43.0	2.72	2.37	2.37	10.9±0.9	11.1±0.9	12.3±1.2	<0.5	<0.5	<0.5	15.3±2.6	17.2±2.5	21.4±2.5
44–46	43.5	39.8	42.3												
46–48	39.6	39.1	38.6												
48–50	37.7	39.8	37.3	2.2	2.24	2.1	9.4±0.8	9.8±0.8	11.9±1.3	<0.5	<0.5	<0.5	20.1±2.7	18.8±2.7	18.7±2.1
50–52	37.6	39.7	38.9												
52–54	39.9	40.0	39.7						10.6±1						
54–56	40.0	40.8		2.04	2.27		10.2±1.1	10.8±1.0		<0.5	<0.5		18±2.07	16.5±2.6	

Table 4
Pb, Zn, Cd, Hg

z (cm)	Pb (ppm)			Zn (ppm)			Cd (ppm)			Hg (ppm)		
	S1	S2	S3	S1	S2	S3	S1	S2	S3	S1	S2	S3
0–2	35.3	35.8	43.5	141	132	97.9	0.5	0.41	0.21	0.30	0.32	0.51
2–4												
4–6												
6–8	44.5	40.6	46.2	157	130	108	0.55	0.42	0.15	1.09	0.34	0.31
8–10												
10–12												
12–14	40.0	31.2	41.2	129	78.6	112	0.54	0.15	0.11	0.26	0.30	0.46
14–16												
16–18												
18–20	29.3	25.5	24.8	79.4	69.2	81.1	0.21	0.15	0.10	0.14	0.37	0.58
20–22												
22–24												
24–26	19.6	29.6	24.9	69.2	78.5	78.8	0.16	0.17	0.05	0.24	0.29	0.19
26–28												
28–30												
30–32	18.5	21.6	22.0	59.0	78.7	75.7	0.11	0.15	0.13	0.08	0.10	0.09
32–34												
34–36												
36–38	21.4	18.2	20.3	67.4	63.4	65.2	0.16	0.12	0.04	<0.07		<0.07
38–40												
40–42												
42–44	18.2	17.4	23.2	66.9	55.1	66.0	0.06	0.12	0.08	<0.07	<0.07	<0.07
44–46												
46–48												
48–50	10.8	18.6	12.4	57.2	61.7	58.0	0.11	0.17	0.11	<0.07	<0.07	<0.07
50–52												
52–54												
54–56	14.4	18.7		50.5	52.0		0.10	0.11		<0.07		

of the sediments must follow the same order, with a smaller grain size for S1 and greater for S3. This must affect, as it will be seen below, the profile of the rest of the variables. As a whole, it can be appreciated that the water content in the column, a simple measurable variable, provides very useful information about the sedimentary environment.

4.1.2. Organic carbon

The value of OC is within the interval 2–5%, characteristic of muddy estuary sediments. The profile of the OC with respect to the depth presents an analogous form to that of the water: OC is diminishing in the stations S1 and S2 and it remains practically constant at the station S3. Also, the parameter is greater for S1 and smaller for S3, as a consequence of the affinity of the organic matter with the smaller size sediment. Stations S1 and S2 show a superficial value of OC that seems to be smaller than the value that would be expected from the approximately linear trend of the deepest layers. These results indicate a complex interaction in the water–sediment interface that is also responsible for the unusually low values shown by other variables in the layers next to such interface. All the stations have the same organic carbon content for $z > 40$ cm, because

the interface dynamics and the grain size do not have influence at this depth.

4.1.3. ^{210}Pb

The ^{210}Pb activity is within the interval 10–40 Bq/kg, and there is a characteristic exponential by decreasing profile of this radionuclide due to decay of the ^{210}Pb (unsupported) in the deepest (and so more ancient) layers. The ^{210}Pb stays constant below a half metre depth, since it is in secular equilibrium with its progenitor, ^{226}Ra . Furthermore, the equilibrium value is the same at the three stations, $^{210}\text{Pb}_{\text{eq}} = 10 \pm 0.5$ Bq/kg, as consequence of the mineral homogeneity of the sediments in this zone. The activity of ^{210}Pb , within the first 20 cm, presents the greatest values for the S1 station and the lowest values for the S3 station, due to the affinity of the unsupported lead with the smaller grain size sediment and greater organic content. On the other hand, an unusually low activity is seen within the first layers ($z < 7$ cm) due to the earlier mentioned interface effect.

4.1.4. ^{137}Cs

The activity of ^{137}Cs is below 10 Bq/kg in every station, which is usual in other coastal sediments from analogous latitude. As expected, this radionuclide is

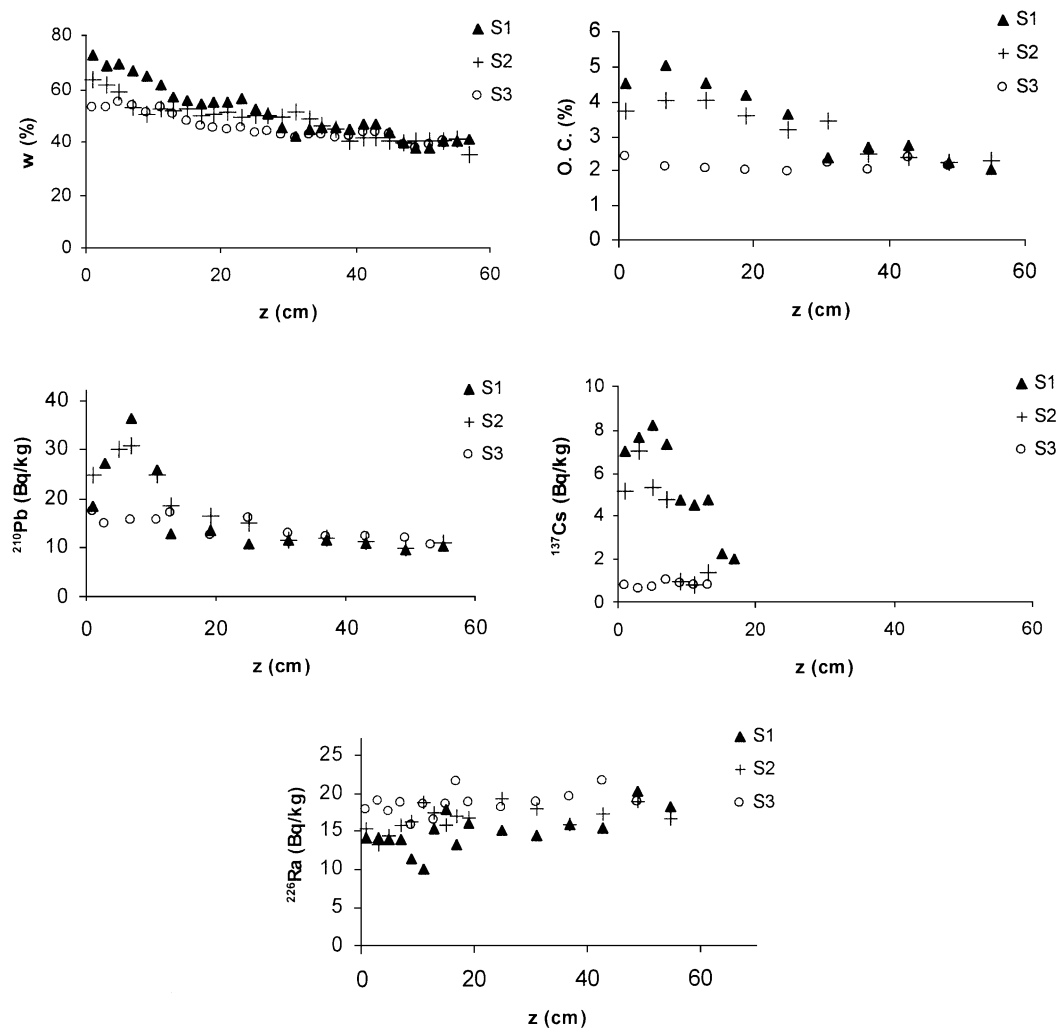


Fig. 2. Depth profiles of w , OC, ^{210}Pb , ^{137}Cs and ^{226}Ra .

only detected in the superficial layers, as a consequence of its recent incorporation to the environment. So, we have found quantities above the minimal detectable activity (MDA) within the first 17 cm of the S1 station column, and up to 14 cm depth for the S2 and S3 stations. The greater activity corresponds to the S1 station and the lower activity to the S3 station, which is due to the affinity of the ^{137}Cs with the smaller grain size sediment. As expected, the activity profile in the columns presents some maxima values, which appear in the 4–6 cm depth layer at the S1 station, and at $z=2$ –4 cm, with a possible second maximum located at $z=14$ cm, at the S2 station. In the case of the station S3, the relative uncertainty of the ^{137}Cs activity is very large, as it corresponds to the very low activity measured (only slightly above the $\text{MDA}=0.6$ Bq/kg) due to the greater grain size of the sediments.

4.1.5. ^{226}Ra

The activity of ^{226}Ra is within the interval 10–20 Bq/kg, as it corresponds to a low radioactive background

zone. The profile of this radionuclide is constant and similar at all the stations, as a consequence of the common geological origin of the sediments (Ramos-Lerate et al., 1998b). The measured activity of ^{226}Ra is slightly greater than the activity found for ^{210}Pb in the deeper levels. It seems that ^{210}Pb is not strictly in secular equilibrium with its parent, may be due to a loss by gaseous emanation of ^{222}Rn , which is an intermediate element of the radioactive chain. Even though the activity of ^{226}Ra will not be used as the equilibrium value for dating, it is useful to know that the activity of this radioisotope is constant, because it is possible to assure that the activity of ^{210}Pb coming from the sediment must also be constant in all the stations, and equal to the value of ^{210}Pb in the deepest layers.

4.1.6. Pb

The measured concentration of this metal is in the range 10–45 ppm, and decreases with respect to the depth in all the stations. The greater concentrations are located within the first 15 cm, and below this depth a

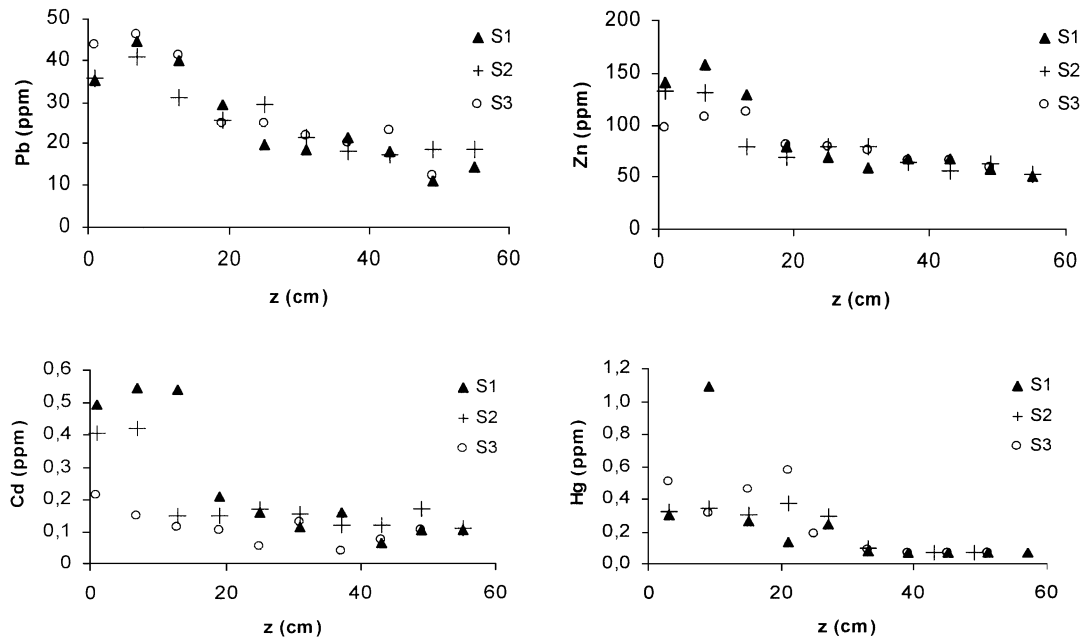


Fig. 3. Depth profiles of Pb, Zn, Cd and Hg.

nearly constant value of 10–20 ppm is reached. Particularly, the decreasing behaviour of Pb at the station S3 demonstrates that this metal is not associated with the organic matter, since in this station the profile of CO is not diminishing. Furthermore, the profiles of Pb for the three stations (Fig. 2) neither show a larger concentration at S1 nor show a smaller concentration at S3. Instead, the profiles are identical in all the stations, which supports the hypothesis that the concentration of the Pb is not associated with the organic content in the sediments. So, the increase of Pb content in the recent layers is due to a greater presence of this metal in the aquatic environment, probably as consequence of the gas emission from vehicles that employ gasoline containing anti-knock based in lead. The bridge over the Bay favours its subsequent transfer to the marine environment, with independence of the grain size and organic content of the sediments. The association between ^{210}Pb and the grain size (and OC) in the sediments points to the radically different origin of this isotope of the Pb. The disintegration of the ^{222}Rn emanated towards the atmosphere produces, through a chain of short life intermediate radioelements, ^{210}Pb . This radioelement is quickly solved by the marine water and is incorporated into the sediments by direct adhesion on the interface, or by fixing into the particles or into the organic matter in suspension that is later deposited on the bottom.

Since the concentration of Pb in deep sediments is around 10–20 ppm, and the maximum values are greater than 40 ppm, we can assert that the concentration of this metal in the sediments has been multiplied by a factor of 2–4. According to the regulation of the

USEPA (United States Environment Protection Agency) for dredged material deposition in the sea, a sediment with a concentration of 40–60 ppm of Pb must be considered *moderately contaminated*, and below this level, pollution is not considered to exist. Therefore, taking into account the Pb concentration in the superficial levels, the stations under study should be considered as *moderately contaminated by Pb*. It can be seen that the concentration in the interface level is lower than the value in the underlying level. This decrease of the concentration of Pb could obey to a decrease in the use of unleaded petrol, but we cannot reject that such decrease can also be a consequence of the interface phenomenon. A more detailed study of this limit layer, as well as the data analysis of the consumption of both types of fuel in the zone over the last years, would clarify this aspect. However, this is not the purpose of this article.

4.1.7. Zn

The concentration of this metal is within the interval 50–150 ppm, and shows a decreasing profile in all the stations. As in the case of Pb, the largest concentrations of Zn appear in the first superficial 15 cm, and from this depth the concentration decreases smoothly to reach a constant value of 50–60 ppm. Again, the decreasing values of Zn in the station S3 indicate that the variation of the concentration is not linked to the organic matter content in the sediments. So, the greater concentration of Zn in the recent sediments is due to the increasing concentration of this metal in the marine water, as consequence of the polluted wastes dumped by the industrial activities in the zone. The concentration of Zn in

the younger sediments has been tripled at station S1 and doubled at S2 and S3 stations. According to the levels established by the USEPA normative, sediments with a concentration of Zn between 90 and 200 ppm are considered as *moderately polluted*. Since the values of Zn in the superficial sediments ($z < 15$ cm) are within such interval, all the studied stations can be catalogued as moderately polluted by Zn.

From the profiles of Zn, a slightly different concentration of this metal is found in the most superficial layers of the three stations, which seems to be related to the different grain size of the sediments. This fact indicates that the Zn has affinity with the sediment, depending on its grain size and OC content. Nevertheless, due to the reduced effect that it provokes, it is a secondary problem.

4.1.8. Cd

The concentration of this metal is within the interval 0.05–0.5 ppm and, in all the stations, it shows a decreasing profile. In the Fig. 3 we can see that the highest concentration of Cd is located in the superficial layers with the smallest grain size. Therefore, it seems that the profile of this metal is not representative of its historical evolution. Instead, this profile seems to show the diffusion of the element through the sedimentary column from the aquatic environment and the interface towards deeper layers, and its fixation affinity with the organic matter. The concentration of Cd in the superficial layers with respect to its value in the deepest layers increases by a factor of 5 at S1 station, 4 at S2 station and 2 at S3 station. Nevertheless, none of the three stations can be considered as polluted by Cd, in terms of the USEPA normative, which establishes the concentration interval of 1–6 ppm for moderately Cd polluted sediments.

4.1.9. Hg

The concentration of this metal is below 1 ppm, showing a decreasing profile. The station S1 shows the interface effect clearly. So, in the shallow layers (up to 20 cm) of the S3 station, there exists a dispersion of the values, whereas at the S2 station, a plateau with a constant concentration of around 0.3 ppm is observed. For intermediate layers ($z > 20$ cm), the Hg decreases, whereas in the deepest layers of all the stations the concentration falls below the detection limit (0.07 ppm). All the stations are in the concentration interval 0.3–1 ppm, which is considered as *moderately polluted by Hg* as the USEPA normative. No relationship with the grain size of the sediments is seen.

4.2. Time evolution of the pollution

In Fig. 4, the concentrations of the heavy metals Pb, Zn, Cd and Hg are plotted versus the time. Also, the

measured activity of ^{137}Cs is represented, in order to verify whether this radionuclide provides additional information about the dating obtained through the ^{210}Pb method.

It can be emphasized that the concentration of Pb as a function of the time has a very similar shape for the three stations. It shows a slight growth until the middle of the nineteenth or the beginning of the twentieth centuries, and from this date the increase has been more significant. During the second half of the twentieth century, the concentration of this metal has exceeded the threshold of the moderate pollution level (40 ppm). Nevertheless, this concentration is diminishing in the most recent layers, younger than 15 years old, which could indicate a smaller presence of Pb in the aquatic environment, probably due to the increasing use of Pb free gasoline.

The evolution of Zn is similar to the Pb. So, the Zn contents increase smoothly in all the stations until the beginning or the middle of the twentieth century, and since then increases more strongly. It seems that the pollution by Zn is a more recent phenomenon than the pollution associated with Pb. Again, a decrease in the concentration of Zn is seen in the most recent layers of the S1 and S3 stations.

To the contrary, it seems that a recent contribution of Cd has taken place in the aquatic environment, as is demonstrated by the greater concentration of this metal in the younger layers of S1 and S3 stations. However, we have already discussed the probable diffusion of Cd towards the deepest layers and its supposed affinity with the small grain size sediments and the organic matter. Therefore, the profile of Cd in the column does seem to indicate adequately the time evolution with the concentration of this metal.

Finally, the concentration of the Hg remains constant or below the detection level until the second half of the nineteenth century or the beginning of the twentieth century, and from this date until the present time a speed growth of its concentration is noticed.

Concerning ^{137}Cs in S1 station, this radionuclide is detected in sedimentary layers formed before the year 1954, when it was introduced in the environment. This confirms the great mobility of this element through the interstitial water of the sedimentary column, which provokes its diffusion towards deeper layers. In the most recent levels of this station there appears a maximum activity, dated as the year 1985 ± 1 , which is in agreement with the fallout of this radionuclide on the zone, as a consequence of the disaster of the nuclear reactor of Chernobyl in 1986. The maximum number of ^{137}Cs that would correspond to the year 1962–1963 is not detected, which is probably due to the experimental uncertainty for the deeper layers. In the station S2, there is no activity of ^{137}Cs for the layers formed prior to 1953 ± 5 year, which is in agreement with the

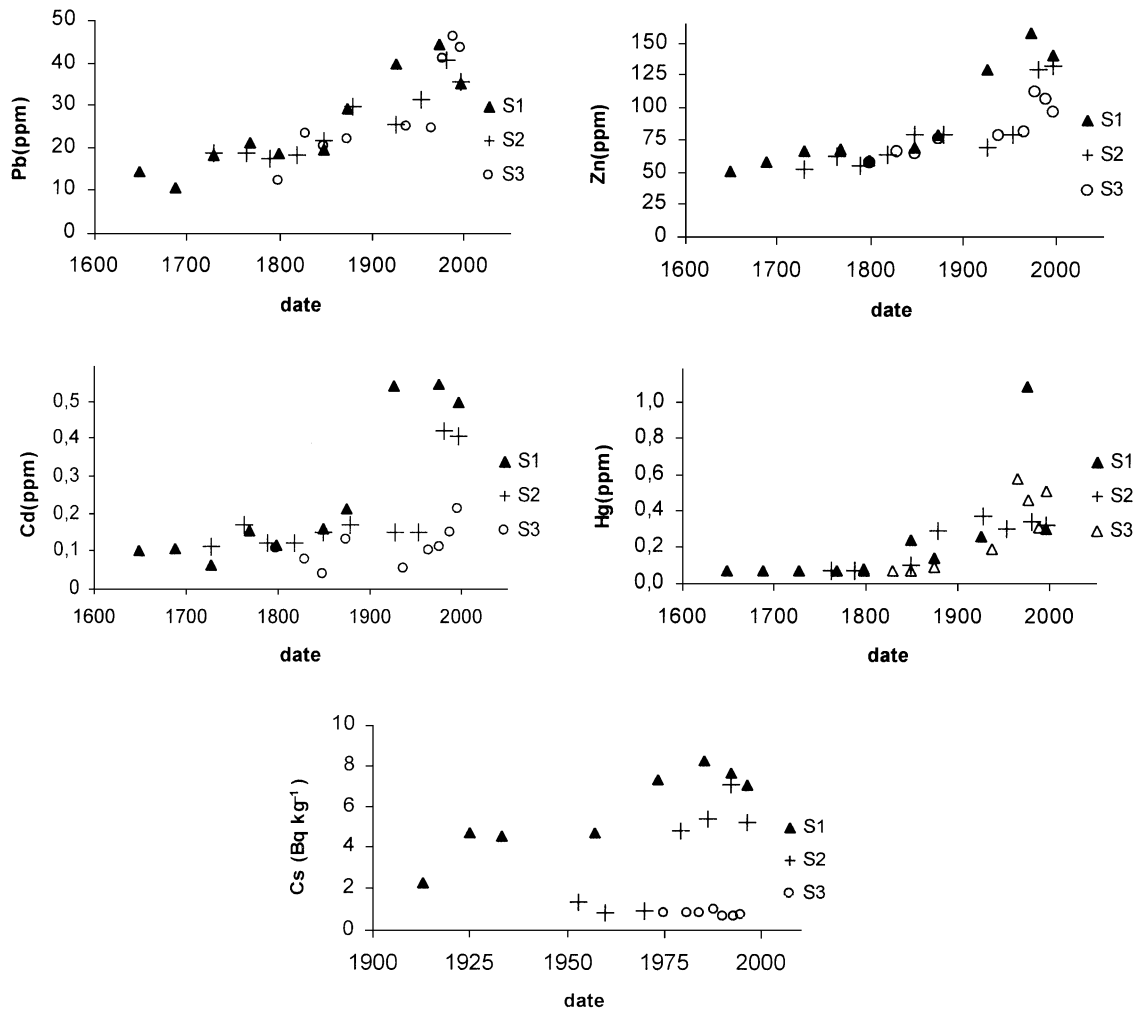


Fig. 4. Trends with time for Pb, Zn, Cd, Hg and ¹³⁷Cs.

date of introduction of this radionuclide. A maximum is detected in a recent level, dated in 1992 ± 1 year, which must be associated with the event of Chernobyl in 1986, and the maximum associated to the year 1962–1963 is not found, probably due to the above mentioned experimental uncertainty. Finally, the measured activities of ¹³⁷Cs in the S3 station are only slightly above the MDA (0.6 Bq/kg) in the layers formed after the date 1978 ± 1 . In spite of the experimental uncertainty for this station, a maximum is seen in a level corresponding to the date 1988 ± 2 , which could be related to the accident of Chernobyl. Therefore, all the caesium measured in the extracted sediment cores seems to have this origin, so that the activity found below the maximum would be a consequence of the diffusion towards deeper layers.

The presence of ¹³⁷Cs in more modern layers can be explained taking into account its gradual incorporation to the sediments due to the long residence time of this element in the aquatic environment, and its delayed incorporation to the sediment of the sea bed.

5. Conclusions

This research shows that the concentration of the heavy metals in the Bay of Cádiz shows an increase, especially in the second half of the twentieth century, as a consequence of the industrial activities and the urban wastes. So, the Pb, Zn and Hg metals exceed the amount of concentration considered as “moderately polluted” by the USEPA normative. The profile of such metal concentration with respect to the depth can be used to study the time evolution over the last centuries. The concentration of metal Cd seems to be increasing, but it does not exceed the threshold of moderate pollution. However, this profile cannot be used as an indication of the evolution of the Cd concentration, because of its diffusion through the sedimentary column.

The sedimentation rates in the Bay of Cádiz are around $100 \text{ mg}/(\text{cm}^2 \text{ year})$, corresponding to an accumulated amount of around $0.2 \text{ cm}/\text{year}$. The sedimentation rate depends on the hydrodynamics energy of

the marine environment, *increasing the sedimentation rate with the energy*.

It has been shown that the profiles with respect to the depth of the parameters water and organic carbon contents, parameters linked to the sediment grain size, are useful to classify the energetic conditions of each station.

Although the ^{210}Pb technique applied to dating sediments is effective and precise, and the analysis of ^{137}Cs is useful to corroborate its results, the application of these methods to an estuary should be done carefully, since the dynamic conditions in such systems usually determine a relatively poor accumulation of such radioelements into marine sediments.

References

- Abril, J.M., García-León, M., García-Tenorio, R., Sánchez, C.I., El-Daoushy, F., 1992. Dating of marine sediments bay and incomplete mixing model. *J. Environ. Radioactivity* 15, 135–151.
- Appleby, P.G., Olfield, F., 1983. The assessment of Pb-210 data from sites with varying sediment accumulation rates. *Hydrobiologia* 103, 29–35.
- Barragán, J.M., 1995. Puerto, Ciudad y Espacio litoral de la Bahía de Cádiz. Salamanca, Varona.
- Barragán, J.M., 1996. Estudios para la ordenación, planificación y gestión integradas en las zonas húmedas de la Bahía de Cádiz. Oikos-Tav S.L, Barcelona.
- Barrera, M., Ramos-Lerate, I., Ligeró, R.A., Casas-Ruiz, M., 1999. Optimization of samples height in cylindrical geometry for gamma spectrometry measurements. *Nucl. Instrum. and Methods in Physics Research A* 421, 163–175.
- Callaway, J.C., DeLaune, R.D., Patrick, W.H., 1996. Chernobyl Cs-137 used to determine sediment accretion rates at selected northern European coastal wetlands. *Limnol. Oceanogr.* 41 (3), 444–450.
- Clifton, R.J., Watson, P.G., Davey, J.T., Frickers, P.E., 1994. A study of processes affecting the uptake of contaminants by intertidal sediments, using the radioactive tracers. *Estuarine, Coastal and Shelf Science* 41, 459–474.
- Consejería de Agricultura y Pesca (Junta de Andalucía), 1994. El medio físico y biológico en la bahía interior: saco interior.
- Davis, R.B., Hess, C.T., Norton, S.A., Hanson, D.W., Hoagland, K.D., Anderson, D.S., 1984. ^{137}Cs and ^{210}Pb dating of sediments from soft-water lakes in New England (USA) and Scandinavia, a failure of ^{137}Cs dating. *Chem. Geol.* 44, 151–185.
- Dickinson, W.W., Dunbar, G.B., McLeod, H., 1996. Heavy metal history from cores in Wellington Harbour, New Zealand. *Environmental Geology* 27, 59–69.
- El-Rayis, O.A., 1985. Re-assessment of the tritiation method for the determination of organic carbon in recent sediments. *Rapp. Comm. Int. Mer Médit.* 29, 45–47.
- Gaudette, H.E., Flight, W.R., Toner, L., Folger, D.W., 1974. An inexpensive tritiation method for the determination of organic carbon in recent sediments. *Journal of Sedimentary Petrology* 44, 249–253.
- Pinglot, J.F., Pourchet, M., 1995. Radioactivity measurements applied to glaciers and lake sediments. *The Science of the Total Environment* 173, 211–223.
- Ramos-Lerate, I., Barrera, M., Ligeró, R.A., Casas-Ruiz, M., 1998a. A new method for gamma-efficiency calibration of voluminal samples in cylindrical geometry. *J. Environ. Radioact.* 38, 47–57.
- Ramos-Lerate, I., Barrera, M., Ligeró, R.A., Casas-Ruiz, M., 1998b. Radionuclides in the environment of the Bay of Cádiz. *Radiation Protection Dosimetry* 75, 41–48.
- Sturgeon, R.E., Desaulniers, J.A.H., Berman, S.S., Russell, D.S., 1982. Determination of trace metals in estuarine sediments by graphite-furnance atomic absorption spectrometry. *Analytica Chimica Acta* 134, 238–291.